Approach to calculation of mass spectra and two-photon decays of $c\bar{c}$ mesons in the framework of Bethe-Salpeter equation

Shashank Bhatnagar[1,*] and Lmenew Alemu[2,†]

[1]Department of Physics, University Institute of Sciences, Chandigarh University, Mohali-140413, India
[2]Department of Physics, Addis Ababa University, P.O.Box 1176 Addis Ababa, Ethiopia

(Received 17 October 2017; revised manuscript received 19 December 2017; published 21 February 2018)

In this work we calculate the mass spectra of charmonium for $1P, \ldots, 4P$ states of 0^{++} and 1^{++}, for $1S, \ldots, 5S$ states of 0^{-+}, and for $1S, \ldots, 4D$ states of 1^{--} along with the two-photon decay widths of the ground and first excited states of 0^{++} quarkonia for the process $O^{++} \to \gamma\gamma$ in the framework of a QCD-motivated Bethe-Salpeter equation (BSE). In this 4×4 BSE framework, the coupled Salpeter equations are first shown to decouple for the confining part of the interaction (under the heavy-quark approximation) and are analytically solved, and later the one-gluon-exchange interaction is perturbatively incorporated, leading to mass spectral equations for various quarkonia. The analytic forms of wave functions obtained are used for the calculation of the two-photon decay widths of χ_{c0}. Our results are in reasonable agreement with data (where available) and other models.

DOI: 10.1103/PhysRevD.97.034021

I. INTRODUCTION

An important role in applications of QCD to hadronic physics is played by charmonium ($c\bar{c}$) and bottomonium ($b\bar{b}$), which are built from a heavy quark and heavy antiquark. By definition, a heavy quark has a mass m, which is large in comparison to the typical hadronic scale Λ_{QCD}. Quarkonium systems are crucially important to improving our understanding of QCD. Heavy-light mesons are much more complicated, as here one really tests the wide range of soft, hard, and soft-collinear scales [1]. The ground-state quarkonia, on the other hand, have been shown over the past decade to be rather well described in nonrelativistic QCD and nonrelativistic potential models.

There has a been a renewed interest in recent years in the spectroscopy of these heavy hadrons in the charm and beauty sectors, which was primarily due to experimental facilities around the world—such as *BABAR*, Belle, CLEO, DELPHI, and BES [2–6]—which have been providing accurate data on $c\bar{c}$ and $b\bar{b}$ hadrons with respect to their masses and decays. In the process, many new states have been discovered, such as $\chi_{b0}(3P)$, $\chi_{c0}(2P)$, $X(3915)$, $X(4260)$, $X(4360)$, $X(4430)$, and $X(4660)$ [6]. The data strongly suggests that among these new resonances there may be exotic four-quark states, hybrid states with gluonic degrees of freedom in addition to a $c\bar{c}$ pair, or loosely bound states of heavy hadrons, i.e., charmonium molecules. Further, there are also open questions about the quantum number assignments of some of these states such as $X(3915)$ [as to whether it is $\chi_{c0}(2P)$ or $\chi_{c2}(2P)$ [7,8]]. Thus, charmonium offers us intriguing puzzles.

However, since the mass spectrum and the decays of all of these bound states of heavy quarks can be tested experimentally, theoretical studies on them may provide valuable insight about the heavy-quark dynamics and lead to a deeper understanding of QCD. Studies of the mass spectrum of these hadrons are particularly important as they shed light on the $Q\bar{Q}$ potential, since the long-range confinement potential has not been derived from QCD so far. Further, though these states appear to be simple, their production mechanism is still not properly understood. These mesons are involved in a number of reactions which are of great importance for the study of the Cabibbo-Kobayashi-Maskawa matrix and CP violation. In this paper we also study the two-photon decays of scalar quarkonia, χ_{c0}. These decays are sensitive probes of quarkonium wave functions.

The nonperturbative approaches—such as effective field theory [9], lattice QCD [10–12], chiral perturbation theory [13], QCD sum rules [14,15], nonrelativistic QCD [16], the Bethe-Salpeter equation (BSE) [17–28], and potential models [29–31]—have been employed to study heavy quarkonia. Recent progress in the understanding of nonrelativistic field theories make it possible to go beyond phenomenological models, and for the first time face the possibility of providing a unified description of all aspects of heavy

*Corresponding author.
shashank_bhatnagar@yahoo.com
†lim_alem98@yahoo.com

quarkonium physics. This allows us to use quarkonium as a benchmark for understanding QCD, for a precise determination of Standard Model parameters (e.g., heavy quark masses, the QCD coupling constant, α_s), and for new physics searches.

All of this opens up new challenges in our theoretical understanding of heavy hadrons, and also provides an important tool for exploring the structure of these simplest bound states in QCD and for studying the nonperturbative (long-distance) behavior of strong interactions. The more recent and sophisticated QCD-modeled treatment of the BSE can be found in Refs. [32–42].

In the present work, we calculate the full mass spectra of charmonium for $1P, \ldots, 3P$ states of 0^{++} and 1^{++} and for $1S, \ldots, 4S$ states of 0^{-+} and 1^{--}, along with the two-photon decay widths of the ground and first excited states of scalar quarkonia (χ_{c0}) for the process $O^{++} \to \gamma\gamma$ in the framework of a QCD-motivated Bethe-Salpeter equation under the covariant instantaneous ansatz (CIA), employing the full BS kernel comprising both the long-range confinement and the short-range one-gluon-exchange (Coulomb) interactions.

We do understand that in $Q\bar{Q}$ quarkonia, the constituents are close enough to each other to warrant a more accurate treatment of the Coulomb term. On the other hand, for $b\bar{b}$ systems the Coulomb term will be extremely dominant in comparison to the confining term, and it should not be treated perturbatively. However, given our mass spectral results for $c\bar{c}$ systems, it may not be so unreasonable to treat the Coulomb term perturbatively for $c\bar{c}$ systems. This is especially so for orbital excitations of these states, where the centrifugal effects [43] ensure that the $c-\bar{c}$ separation is large enough to feel the effect of the confining term more strongly than the Coulomb term. We further wish to state that some earlier works [43–45] have treated the one-gluon-exchange (OGE) (Coulomb) term perturbatively for charmed mesons and baryons, while other works [46,47] did not take into account the importance of the Coulomb term for heavy quarkonium systems.

Thus, in the present paper the coupled Salpeter equations for scalar (0^{++}) and axial-vector (1^{++}) quarkonia are first shown to decouple for the confining part of the interaction, under the heavy-quark approximation, and the analytic forms of mass spectral equations are worked out, which are then solved in approximate harmonic oscillator basis to obtain the unperturbed wave functions for various states of these quarkonia. We then perturbatively incorporate the one-gluon-exchange into the unperturbed spectral equation, and obtain the full spectrum. The wave functions of scalar (0^{++}) quarkonia are then used to calculate their two-photon decay widths. We further extend the mass spectral calculations of pseudoscalar (0^{-+}) and vector (1^{--}) quarkonia in Ref. [48] with the perturbative inclusion of one-gluon-exchange effects. The approximations used in this analytic treatment of the confining interaction are shown to be fully under control. This work is an improvement on our earlier work [48] on the mass spectral problem for pseudoscalar and vector states of quarkonia, in line with some of the earlier works [49–51] where we used only the confining interaction.

A quarkonium state is classified by quantum numbers J^{PC}, where $J = L + S$, the parity $P = (-1)^{L+1}$, and the charge conjugation $C = (-1)^{L+S}$. With this classification, the lowest states ($l = 0$) are present in 0^{-+} (pseudoscalar) quarkonia, while the lowest state ($l = 0$) and the second orbitally excited ($l = 2$) state are present in 1^{--} (vector) quarkonia. However, the first orbitally excited ($l = 1$) states are present in 0^{++} (scalar) and 1^{++} (axial-vector) quarkonia. The same holds true for their radial excitations.

This paper is organized as follows. Section II deals with the mass spectral calculations of the ground and excited states of 0^{++} quarkonia. Section III deals with the mass spectral calculation of the ground and excited states of 0^{-+} and 1^{--} quarkonia, while Sec. IV deals with the mass spectral calculations of the ground and excited states of 1^{++} quarkonia. Section V deals with the calculation of the two-photon decay widths of χ_{c0}. Section VI contains our numerical results and discussions.

II. FORMULATION OF THE BSE UNDER THE CIA

Here we cover the main points of the BSE under the CIA, which is a Lorentz-invariant generalization of instantaneous approximation, which is used to derive the three-dimensional (3D) Salpeter equations. We start with a four-dimensional (4D) BSE for a $q\bar{q}$ system with quarks of constituent masses m_1 and m_2, written in a 4×4 representation of the 4D BS wave function $\Psi(P,q)$ as

$$S_F^{-1}(p_1)\Psi(P,q)S_F^{-1}(-p_2) = \frac{i}{(2\pi)^4}\int d^4q' K(q,q')\Psi(P,q'), \tag{1}$$

where $K(q,q')$ is the interaction kernel between the quark and antiquark, and $p_{1,2}$ are the momenta of the quark and antiquark, which are related to the internal 4-momentum q and total momentum P of a hadron of mass M as $p_{1,2\mu} = \hat{m}_{1,2}P_\mu \pm q_\mu$, where $\hat{m}_{1,2} = \frac{1}{2}[1 \pm \frac{(m_1^2-m_2^2)}{M^2}]$ are the Wightman-Garding definitions of the masses of individual quarks, which ensure that $P.q = 0$ on the mass shells of each quark, i.e., $p_1^2 + m_1^2 = p_2^2 + m_2^2 = 0$ for both $m_1 = m_2$ and $m_1 \neq m_2$, and $\hat{m}_{1,2}$ reduce to $\hat{m}_{1,2} = \frac{m_{1,2}}{m_1+m_2}$ in the nonrelativistic limit. [These constituent masses $m_{1,2}$ are strictly momentum dependent, since they contain the mass function $m(p)$, but may be regarded as almost constant, $m(p) = m(0)$, for low-energy phenomena.] With these Wightman-Garding definitions, $\hat{m}_{1,2}$ always satisfy $\hat{m}_1 + \hat{m}_2 = 1$, and they are a natural choice that allocates most of the momentum to the heavy quark, while a smaller part of the momentum goes to the lighter quark in a heavy-light meson. However, for equal-mass mesons

(such as in $c\bar{c}$ systems, where $m_1 = m_2 = m$), we have $\hat{m}_1 = \hat{m}_2 = \frac{1}{2}$. Then, $p_{1,2\mu}$ becomes $p_{1,2\mu} = \frac{1}{2}P_\mu \pm q_\mu$ (as in Refs. [37,38]) where the momentum is shared equally between the two quarks.

Now it is convenient to express the internal momentum of the hadron q_μ as the sum of two parts. They are (i) the transverse component $\hat{q}_\mu = q_\mu - (q\cdot P)P_\mu/P^2$, which is orthogonal to the total hadron momentum P_μ [i.e., $\hat{q}\cdot P = 0$ regardless of whether the individual quarks are on-shell $(P.q = 0)$ or off-shell $(P.q \neq 0)$], and (ii) the longitudinal component $\sigma P_\mu = (q\cdot P)P_\mu/P^2$, which is parallel to P_μ. Thus, we can decompose q_μ as $q_\mu = (\hat{q}, iM\sigma)$, where the transverse component $\hat{q}$ is an effective 3D vector, while the longitudinal component $M\sigma$ plays the role of the time component. It should be noted that, although $\hat{q}_\mu$ is an effective 3D vector, it is indeed a 4-vector, and $\hat{q}^2 = q^2 - (q\cdot P)^2/P^2$ is positive definite throughout the entire 4D space.

The 4D volume element in this decomposition is $d^4q = d^3\hat{q}Md\sigma$. To obtain the 3D BSE and the hadron-quark vertex, we use an ansatz on the BS kernel K in Eq. (1) which is assumed to depend on the 3D variables $\hat{q}_\mu$, $\hat{q}'_\mu$ as

$$K(q,q') = K(\hat{q},\hat{q}'). \tag{2}$$

Hence, the longitudinal component $M\sigma$ of q_μ does not appear in the form $K(\hat{q},\hat{q}')$ of the kernel. To reduce Eq. (1) to a 3D form, we define the 3D wave function $\psi(\hat{q})$ as

$$\psi(\hat{q}) = \frac{i}{2\pi}\int Md\sigma\Psi(P,q). \tag{3}$$

Substituting Eq. (5) into Eq. (1), with the definition of the kernel in Eq. (4), we get a covariant version of the Salpeter equation,

$$(i\not{p}_1 + m_1)\Psi(P,q)(-i\not{p}_2 + m_2) = \int \frac{d^3\hat{q}'}{(2\pi)^3}K(\hat{q},\hat{q}')\psi(\hat{q}'), \tag{4}$$

and the 4D BS wave function becomes

$$\Psi(P,q) = S_F(p_1)\Gamma(\hat{q})S_F(-p_2), \tag{5}$$

where

$$\Gamma(\hat{q}) = \int \frac{d^3\hat{q}'}{(2\pi)^3}K(\hat{q},\hat{q}')\psi(\hat{q}') \tag{6}$$

plays the role of the hadron-quark vertex function, which satisfies a 4D BSE with a natural off-shell extension over the entire 4D space (due to the positive definiteness of the quantity $\hat{q}^2$), and thus provides a fully Lorentz-invariant basis for the evaluation of various transition amplitudes through various quark loop diagrams. Here due to $\gamma_\mu \otimes \gamma_\mu$ form of the kernel, details of which are given in [48], we can write $\Gamma(\hat{q}) = \int \frac{d^3\hat{q}'}{(2\pi)^3}V(\hat{q},\hat{q}')\gamma_\mu\psi(\hat{q}')\gamma_\mu$ (where V is spatial part of the kernel), where we can to a good approximation express $\gamma_\mu\psi(\hat{q}')\gamma_\mu \approx \Theta\psi(\hat{q}')$, where Θ involves the spin-spin interactions alone, on taking the dominant Dirac structures in $\psi(\hat{q}')$ in Eq. (9), and ignoring terms like $\hat{q}^2/M^2$ in expressions for hadron-quark vertex function, $\Gamma(\hat{q})$ and the full 4D BS wave function, $\Psi(P,q)$ in Eqs. (6), and (5) respectively that have negligible contributions in the heavy-quark limit. Following a sequence of steps outlined in Ref. [48], we get the covariant forms of the Salpeter equations (in the 4D variable $\hat{q}$), which are effective 3D forms of the BSE and are valid for hadrons in arbitrary motion. The complete 3D BS wave function is a 4×4 matrix in spinor space, and separates into four parts as [21,48] $\psi(\hat{q}) = \psi^{++}(\hat{q}) + \psi^{+-}(\hat{q}) + \psi^{-+}(\hat{q}) + \psi^{--}(\hat{q})$, where each of these is a 4×4 matrix.

The four independent Salpeter equations are [21,48]

$$\begin{aligned}
(M-2\omega)\psi^{++}(\hat{q}) &= -\Lambda_1^+(\hat{q})\Gamma(\hat{q})\Lambda_2^+(\hat{q}),\\
(M+2\omega)\psi^{--}(\hat{q}) &= \Lambda_1^-(\hat{q})\Gamma(\hat{q})\Lambda_2^-(\hat{q}),\\
\psi^{+-}(\hat{q}) &= 0,\\
\psi^{-+}(\hat{q}) &= 0,
\end{aligned} \tag{7}$$

where $\Lambda^\pm$ are the projection operators [48] for each of the constituents. The framework is quite general so far. Thus, to obtain the mass spectral equation we have to start with the above four equations to solve the instantaneous BS equation.

III. MASS SPECTRA OF SCALAR QUARKONIA

We start with the most general decomposition of a 4D BS wave function for a scalar meson [17,19],

$$\begin{aligned}
\psi(P,q) = {} & f_1(q,P) - i\not{P}f_2(q,P) - i\not{q}f_3(q,P)\\
& - [\not{P},\not{q}]f_4(q,P),
\end{aligned} \tag{8}$$

which is expressible as a linear superposition of four Dirac covariants, each multiplied by a Lorentz scalar amplitude f_i that have different dimensions of mass. We first reexpress $\psi(P,q)$ by making these amplitudes $f_i(q,P)$ dimensionless by weighing each Dirac structure by an appropriate power of the meson mass M. Thus, each term in the expansion of $\psi(P,q)$ is associated with a certain power of M [25,27]. Further, making use of the 3D reduction, and making use of the fact that $\hat{q}.P = 0$, we can write the general decomposition of the instantaneous BS wave function for scalar mesons $(J^{pc} = 0^{++})$ of dimensionality M as

$$\psi(\hat{q}) = Mf_1(\hat{q}) - i\not{P}f_2(\hat{q}) - i\tilde{\not{q}}f_3(\hat{q}) - \frac{2\not{P}\tilde{\not{q}}}{M}f_4(\hat{q}). \tag{9}$$

Until now these amplitudes have all been independent, and per the power-counting rule [25–27] proposed by us earlier, f_1 and f_2 are the amplitudes associated with the leading Dirac structures, namely, M and $\not{P}$, while f_3 and f_4 will be the amplitudes associated with the subleading Dirac structures, namely, $\tilde{\not{q}}$, and $\frac{2\not{P}\tilde{\not{q}}}{M}$.

We now use the last two Salpeter equations, that act as two constraint conditions $\psi^{+-}(\hat{q}) = 0$, and $\psi^{-+}(\hat{q}) = 0$ in the 3D Salpeter equations, Eq. (7). Due to these two equations, the scalar functions $f_i(\hat{q})(i = 1, \ldots, 4)$ are no longer independent, but rather are tied together by the relations (for the equal-mass case)

$$f_1(\hat{q}) = \frac{-\hat{q}^2 f_3(\hat{q})}{Mm},$$
$$f_2(\hat{q}) = 0. \tag{10}$$

Thus, after applying the constraint conditions, the amplitudes get mixed up, and the distinction between the leading and subleading Dirac structures (which was applicable when amplitudes were independent) gets lost.

This is in contrast to the BSE approach [27] [involving the 16×1 structure of the two-body BS amplitude $\Psi(P, q)$], which leads to an exact connection [27] between the 3D and 4D forms of the BSE. After the 3D reduction, we get a single 3D Salpeter equation [as in Eq. (30) of Ref. [27]], and the 3D BS amplitudes (f_is) remain independent, and thus they remain classified in terms of leading and subleading amplitudes.

However, as mentioned above, with the present BSE approach [which involves the 4×4 BS amplitude $\Psi(P, q)$] used in this paper we get four Salpeter equations, and due to the last two Salpeter equations (acting as constraint conditions) the amplitudes get mixed up, and this distinction between leading and subleading amplitudes is lost. Further, the second constraint condition leads to $f_2 = 0$ only on account of equal-mass quarks. Such linkages between BS amplitudes have been obtained before in Ref. [52].

Thus, the relativistic 3D Salpeter wave function of the 0^{++} meson is determined by only two independent scalar functions [f_1 (or f_3) and f_4] in the form

$$\psi(\hat{q}) = \left[\frac{-\hat{q}^2}{m} - i\hat{\not{q}}\right] f_3(\hat{q}) - \frac{2\not{P}\hat{\not{q}}}{M} f_4(\hat{q}) \tag{11}$$

(the same is true for the 0^{-+}, 1^{--}, and 1^{++} mesons). Here, we should note that by using the above constraint equations, we have reexpressed f_1 in terms of f_3. Putting the wave function in Eq. (11) above—along with the projection operators defined in Eq. (13) of Ref. [48]—into the first two Salpeter equations in Eq. (7), and by taking the trace on both sides, we obtain the equations

$$(M - 2\omega)\left[f_3(\hat{q}) + \frac{2mf_4(\hat{q})}{\omega}\right] = \frac{1}{\omega^2\hat{q}^2}\int \frac{d^3\hat{q}'}{(2\pi)^3} K(\hat{q}, \hat{q}')[\hat{q}^2\hat{q}'^2 f_3(\hat{q}') - m^2\hat{q}.\hat{q}' f_3(\hat{q}') - 2m\omega\hat{q}.\hat{q}' f_4(\hat{q}')],$$
$$(M + 2\omega)\left[f_3(\hat{q}) - \frac{2mf_4(\hat{q})}{\omega}\right] = \frac{1}{\omega^2\hat{q}^2}\int \frac{d^3\hat{q}'}{(2\pi)^3} K(\hat{q}, \hat{q}')[-\hat{q}^2\hat{q}'^2 f_3(\hat{q}') + m^2\hat{q}.\hat{q}' f_3(\hat{q}') - 2m\omega\hat{q}.\hat{q}' f_4(\hat{q}')]. \tag{12}$$

The solution of these equations needs information about the BS kernel $K(\hat{q}, \hat{q}')$ [27,48], which is taken to be one-gluon-exchange-like as regards the color $(\frac{1}{4}\vec{\lambda}_1.\vec{\lambda}_2)$ and spin $(\gamma_\mu \otimes \gamma_\mu)$ dependence, while the potential $V(\hat{q}, \hat{q}')$ involves the scalar structure of the gluon propagator in the perturbative (o.g.e), as well as the nonperturbative (confinement) regimes and is given as

$$K(q, q') = \left(\frac{1}{2}\vec{\lambda}_1.\frac{1}{2}\vec{\lambda}_2\right)(\gamma_\mu \otimes \gamma^\mu)V(q - q'),$$
$$V(\hat{q}, \hat{q}') = \frac{4\pi\alpha_s}{(q - q')^2} + \frac{3}{4}\omega_{q\bar{q}}^2 \int d^3\vec{r}\left[r^2(1 + 4\hat{m}_1\hat{m}_2 A_0 M_>^2 r^2)^{-\frac{1}{2}} - \frac{C_0}{\omega_0^2}\right] e^{i(\hat{q}-\hat{q}').\vec{r}}, \tag{13}$$

where $\omega_{q\bar{q}}^2 = 4M\hat{m}_1\hat{m}_2\omega_0^2\alpha_s(M^2)$ is the flavor-dependent spring constant, and the QCD coupling constant $\alpha_s(M^2) = \frac{12\pi}{33-2n_f}[\log(\frac{M^2}{\Lambda^2})]^{-1}$. Here, the proportionality of $\omega_{q\bar{q}}^2$ on $\alpha_S(Q^2)$ is needed to provide a more direct QCD motivation [18,25] to confinement, and ω_0^2 is postulated as a spring constant which is common to all flavors, and is introduced as an input parameter. $A_0 \ll 1$ has been introduced to create a smooth transition from harmonic to linear confinement as one goes from $q\bar{q}$ to $Q\bar{Q}$ systems. C_0 is a dimensionless constant. The full structure of the scalar function V is the sum of one-gluon-exchange, V_{OGE}, and the confining part, V_c. We first ignore the V_{OGE} term, and work only with the confining part V_c in Eq. (13), and write Eq. (12) as

$$(M - 2\omega)\left[f_3(\hat{q}) + \frac{2mf_4(\hat{q})}{\omega}\right] = \frac{\Theta_s}{\omega^2\hat{q}^2}\int \frac{d^3\hat{q}'}{(2\pi)^3} V_c(\hat{q}, \hat{q}')[\hat{q}^2\hat{q}'^2 f_3(\hat{q}') - m^2\hat{q}.\hat{q}' f_3(\hat{q}') - 2m\omega\hat{q}.\hat{q}' f_4(\hat{q}')],$$
$$(M + 2\omega)\left[f_3(\hat{q}) - \frac{2mf_4(\hat{q})}{\omega}\right] = \frac{\Theta_s}{\omega^2\hat{q}^2}\int \frac{d^3\hat{q}'}{(2\pi)^3} V_c(\hat{q}, \hat{q}')[-\hat{q}^2\hat{q}'^2 f_3(\hat{q}') + m^2\hat{q}.\hat{q}' f_3(\hat{q}') - 2m\omega\hat{q}.\hat{q}' f_4(\hat{q}')], \tag{14}$$

where the spin dependence of the interaction is contained in the factor $\Theta_S = \gamma_\mu \psi(\hat{q}) \gamma_\mu$ [48]. The scalar part of the confining potential (which involves the color factor $\frac{1}{2}\vec{\lambda}_1 . \frac{1}{2}\vec{\lambda}_2 = -\frac{4}{3}$) is taken to be [48] $V_c(\hat{q}, \hat{q}') = \bar{V}_c \delta^3(\hat{q} - \hat{q}')$, where $\bar{V}_c(\hat{q}, \hat{q}') = \omega_{q\bar{q}}^2 (2\pi)^3 [\kappa \vec{\nabla}_{\hat{q}}^2 + \frac{C_0}{\omega_0^2}]$, and $\kappa = (1 - A_0 M^2 \vec{\nabla}_{\hat{q}}^2)^{-1/2}$. Here $\bar{V}_c$ is the part of V_c without the delta function. To handle these equations, we first integrate them over $d^3\hat{q}'$, performing the delta function integration that arises due to the presence of $V_c(\hat{q}, \hat{q}')$ in the integrand, and get two coupled algebraic equations with $\bar{V}(\hat{q})$ on the rhs. To decouple them, we first add them. Then, we subtract the second equation from the first equation, and get two algebraic equations which are still coupled. Then, from one of the two equations so obtained, we eliminate $f_3(\hat{q})$ in terms of $f_4(\hat{q})$, and plug this expression for $f_3(\hat{q})$ into the second equation of the coupled set so obtained, to get a decoupled equation in $f_4(\hat{q})$. Similarly, we eliminate $f_4(\hat{q})$ from the second equation of the set of coupled algebraic equations in terms of $f_3(\hat{q})$, and plug it into the first equation to get a decoupled equation entirely in $f_3(\hat{q})$. Thus, we get two identical decoupled equations: one entirely in $f_3(\hat{q})$, and the other entirely in $f_4(\hat{q})$. The calculation up to this point has not used any approximations. However, we notice that if we employ the approximation $\omega \approx m$ on rhs of the two algebraic equations[1] [this is justified since in the confinement region, the relative momentum between heavy quarks in the bound state can be considered small, since the heavy quark is expected to move with nonrelativistic speeds (see Ref. [53]), and these quarks can be treated as almost on mass shell], these decoupled equations can be expressed as

$$\left[\frac{M^2}{4} - m^2 - \hat{q}^2\right] f_3(\hat{q}) = -m\Theta_s \bar{V}_c f_3(\hat{q}) + \frac{\Theta_s^2 \bar{V}_c^2 f_3(\hat{q})}{4},$$
$$\left[\frac{M^2}{4} - m^2 - \hat{q}^2\right] f_4(\hat{q}) = -m\Theta_s \bar{V}_c f_4(\hat{q}) + \frac{\Theta_s^2 \bar{V}_c^2 f_4(\hat{q})}{4}. \tag{15}$$

We see that we get two identical decoupled equations which resemble the harmonic oscillator equations, except for the term involving $\bar{V}_c^2$ on the right-hand side of these equations.

[1]In principle, we should solve the decoupled algebraic equations numerically. However, this would not give an explicit dependence of the mass spectra on the principal quantum number N, nor would this give the explicit algebraic forms of wave functions that can be employed to do analytic calculations of various transition amplitudes for different processes. Our approach may lead to a little loss of numerical accuracy, but it does lead to a much deeper understanding of the mass spectral problem. The approximations used by us have been shown to be totally under control. The plots of our algebraic forms of the wave functions for scalar, pseudoscalar, vector, and axial-vector quarkonia are very similar to the corresponding plots of wave functions in Ref. [22] obtained by purely numerical methods, which validates our approach.

TABLE I. Numerical values of the coefficients $\Omega_S = m\Theta_S \omega_{q\bar{q}}^2$, and $\Omega_S' = \frac{\Theta_s^2}{4}\omega_{q\bar{q}}^4$ associated with the terms involving $\bar{V}_c$ and $\bar{V}_c^2$, respectively, for scalar mesons χ_c on the rhs of Eq. (15), and their percentage ratio for the input parameters of our model mentioned above.

	Ω_S	Ω_S'	$\frac{\Omega_S'}{\Omega_S}\%$
χ_{c0}	0.1213	0.0016	1.315

We wish to mention that in this study on the mass spectra of scalar, pseudoscalar, vector, and axial-vector quarkonia good agreement with data on masses and various decay constants/decay widths of the ground and excited states of η_c, η_b, J/Ψ, and Υ is obtained for the input parameters $C_0 = 0.186889$, $\omega_0 = 0.145\,\text{GeV}$, $\Lambda = 0.250\,\text{GeV}$, and $A_0 = 0.01$, along with the input quark mass $m_c = 1.490$ GeV. With these numerical values for the input parameters, we try to determine the numerical values of $\Omega_S = m\Theta_S \omega_{q\bar{q}}^2$, and $\Omega_S' = \frac{\Theta_s^2}{4}\omega_{q\bar{q}}^4$ associated with the terms involving $\bar{V}_c$ and $\bar{V}_c^2$, respectively, for scalar mesons χ_{c0} on the rhs of Eq. (15). We report their percentage ratio in Table I below, where it can be seen that $\omega_{q\bar{q}}^4 \ll \omega_{q\bar{q}}^2$ and hence the second term on the rhs of Eq. (16) contributes $\sim 1\%$ of the first term on the rhs of this equation for $c\bar{c}$, and thus it can be dropped, as in Ref. [48].

Thus, the rhs of both equations in Eq. (15) only has the term $-m\Theta_s \bar{V}_c f_{3,4}(\hat{q})$. Now, using the spatial part $\bar{V}_c$ in Eq. (15), the wave functions f_3, and f_4 satisfy identical 3D BSEs for equal-mass heavy scalar mesons:

$$\left[\frac{M^2}{4} - m^2 - \hat{q}^2\right] f_3(\hat{q}) = -m\Theta_s \omega_{q\bar{q}}^2 \left[\kappa \vec{\nabla}_{\hat{q}}{}^2 + \frac{C_0}{\omega_0^2}\right] f_3(\hat{q}),$$
$$\left[\frac{M^2}{4} - m^2 - \hat{q}^2\right] f_4(\hat{q}) = -m\Theta_s \omega_{q\bar{q}}^2 \left[\kappa \vec{\nabla}_{\hat{q}}{}^2 + \frac{C_0}{\omega_0^2}\right] f_4(\hat{q}), \tag{16}$$

where we have used $\bar{V}(\hat{q}) = (2\pi)^3 \omega_{q\bar{q}}^2 [\kappa \vec{\nabla}_{\hat{q}}^2 + \frac{C_0}{\omega_0^2}]$ [48], with $\kappa = (1 + 2A_0(N + \frac{3}{2}))^{-1/2}$. Thus the solutions of these equations $f_3(\hat{q}) \approx f_4(\hat{q}) (= \phi^s(\hat{q}))$. With the use of the above equality of the amplitudes, and reexpressing f_3 in terms of f_1, the complete wave function $\Psi^s(\hat{q})$ can be expressed as

$$\Psi^s(\hat{q}) = \left[M + i\frac{mM\hat{\not{q}}}{\hat{q}^2} - \frac{2\hat{P}\hat{\not{q}}}{M}\right] \phi^s(\hat{q}). \tag{17}$$

However, it should be noted that even though the reduced Salpeter wave function in Eq. (17) is reduced to a single amplitude ϕ^s, by multiplying a linear combination

of three distinct Dirac structures all three of these Dirac structures will contribute to the calculation of any observable.

We can reduce this equation to the equation for a simple quantum-mechanical 3D harmonic oscillator with coefficients depending on the hadron mass M and total quantum number N. The wave function satisfies the 3D BSE:

$$\left[\frac{M^2}{4} - m^2 - \hat{q}^2\right]\phi(\hat{q}) = -m\Theta_s\omega_{q\bar{q}}^2\left[\kappa\vec{\nabla}_{\hat{q}}{}^2 + \frac{C_o}{\omega_o^2}\right]\phi(\hat{q}). \tag{18}$$

Now, with the use of leading Dirac structures, we can to a good approximation (as in the case of pseudoscalar and vector mesons [48]) express $\Theta_S = 4$. This is due to the fact that $\gamma_\mu\psi(\hat{q})\gamma_\mu \approx \gamma_\mu(Mf_1)\gamma_\mu = 4\psi(\hat{q})$, due to MI (with I being the unit 4×4 matrix) being the most leading Dirac structure in the scalar meson wave function, and the terms with $\hat{q}^2/m^2$ have negligible contributions in the heavy-quark limit, and thus can be dropped. Thus, the above equation can be put in the form

$$\left(\frac{M^2}{4} - m^2 - \hat{q}^2\right)\phi(\hat{q}) = -\beta_s^4\left[\kappa\vec{\nabla}_{\hat{q}}^2 + \frac{C_0}{\omega_0^2}\right]\phi(\hat{q}), \tag{19}$$

which can in turn be expressed as

$$E_s\phi_s = [-\beta_s^4\vec{\nabla}_{\hat{q}}^2 + \hat{q}^2]\phi_s(\hat{q}), \tag{20}$$

where $\beta_s = (\frac{4m\omega_{q\bar{q}}^2}{\sqrt{1+2A_0(N+3/2)}})^{1/4}$ and the total energy of the system is expressed as

$$E = \frac{M^2}{4} - m^2 + \frac{\beta_s^4 C_0}{\omega_0^2}\sqrt{1+2A_0(N+3/2)}. \tag{21}$$

Putting the expression for the Laplacian operator in spherical coordinates, we get

$$\frac{d\phi(\hat{q})}{d\hat{q}^2} + \frac{2}{\hat{q}}\frac{d\phi(\hat{q})}{d\hat{q}} - \frac{l(l+1)\phi(\hat{q})}{\hat{q}^2} + \left(\frac{E}{\beta_s^4} - \frac{\hat{q}^2}{\beta_s^4}\right)\phi(\hat{q}) = 0, \tag{22}$$

where l is the orbital quantum number with the values $l = 0, 1, 2, 3\ldots$, corresponding to $S, P, D, \ldots$ wave states, respectively. This is a 3D harmonic oscillator equation, whose solutions can be found by using the power-series method. Assuming that the solutions of this equation are of the form $\phi(\hat{q}) = h(\hat{q})e^{-\frac{\hat{q}^2}{2\beta_s^2}}$, the above equation can be expressed as

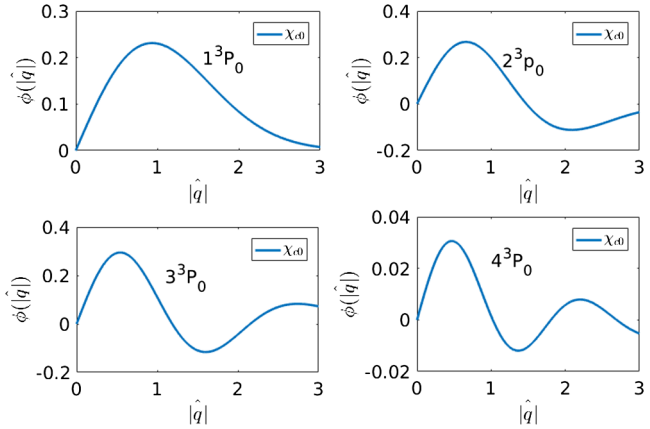

FIG. 1. Plots of wave functions for scalar (0^{++}) quarkonia χ_{c0} Vs $\hat{q}$ (in GeV) for the states $1P$, $2P$, and $3P$.

$$h''(\hat{q}) + \left(\frac{2}{\hat{q}} - \frac{2\hat{q}}{\beta_s^2}\right)h'(\hat{q}) + \left(\frac{E}{\beta_s^4} - \frac{3}{\beta_s^2} - \frac{l(l+1)}{\hat{q}^2}\right)h(\hat{q}). \tag{23}$$

The eigenvalues of this equation can be obtained using the power-series method as

$$E_N = 2\beta_s^2\left[N + \frac{3}{2}\right]; \quad N = 2n + l, \tag{24}$$

with $l = 1$. Thus, to each value of $n = 0, 1, 2, 3, \ldots$ will correspond a polynomial $h(\hat{q})$ of order $2n+1$ in $\hat{q}$, which are obtained as solutions of Eq. (23). The odd-parity normalized wave functions $\phi(\hat{q})$ thus derived are

$$\begin{aligned}
\phi_s(1p,\hat{q}) &= \left(\frac{2}{3}\right)^{1/2}\frac{1}{\pi^{3/4}\beta_s^{5/2}}\hat{q}e^{-\frac{\hat{q}^2}{2\beta_s^2}},\\
\phi_s(2p,\hat{q}) &= \left(\frac{5}{3}\right)^{1/2}\frac{1}{\pi^{3/4}\beta_s^{5/2}}\hat{q}\left[1 - \frac{2}{5}\frac{\hat{q}^2}{\beta_s^2}\right]e^{-\frac{\hat{q}^2}{2\beta_s^2}},\\
\phi_s(3p,\hat{q}) &= \left(\frac{70}{171}\right)^{1/2}\frac{1}{\pi^{3/4}\beta_s^{5/2}}\hat{q}\left[1 - \frac{2\hat{q}^2}{5\beta_s^4} + \frac{4\hat{q}^4}{35\beta_s^4}\right]e^{-\frac{\hat{q}^2}{2\beta_s^2}}\\
\phi_s(4p,\hat{q}) &= \left(\frac{1890}{46359}\right)^{1/2}\frac{1}{\pi^{3/4}\beta_s^{5/2}}\hat{q}\\
&\quad\times\left[1 - \frac{6\hat{q}^2}{5\beta_s^2} + \frac{12\hat{q}^4}{35\beta_s^4} - \frac{24\hat{q}^6}{945\beta_s^6}\right]e^{-\frac{\hat{q}^2}{2\beta_s^2}}.
\end{aligned} \tag{25}$$

The plots of the wave functions for scalar quarkonia χ_{c0} are shown in Fig. 1.

The mass spectrum of ground and excited states for equal-mass heavy scalar (0^{++}) mesons is written as

TABLE II. Mass spectrum in the BSE-CIA of ground and excited states of χ_{c0} with quantum numbers $J^{PC} = 0^{++}$ in units of GeV with the parameter range $\omega \in [0.130\text{–}0.160]$ GeV for the parameter ratio, $\frac{C_0}{\omega_0^2} = 8.8888$ GeV^{-2}, and the other parameters $\Lambda = 0.250$ GeV, $A_0 = 0.01$, and $m_c = 1.490$ GeV. However, for comparison with experiment, we take the values $\omega = 0.145$ GeV and $C_0 = 0.18688$.

	M ($\omega = 0.130$)	M ($\omega = 0.145$)	M ($\omega = 0.160$)	Experiment [6]
$M_{\chi c0}(1p_0)$	3.3967	3.4474	3.4995	3.4140 ± 0.0003
$M_{\chi c0}(2p_0)$	4.0967	4.1552	4.2039	
$M_{\chi c0}(3p_0)$	4.7204	4.8463	4.9687	
$M_{\chi c0}(4p_0)$	5.2961	5.5186	5.7308	

$$\frac{1}{2\beta_s^2}\left(\frac{M^2}{4} - m^2 + \frac{C_0\beta_s^4}{\omega_0^2}\sqrt{1 + 2A_0\left(N + \frac{3}{2}\right)}\right) = N + \frac{3}{2}; \quad N = 2n + l; \quad n = 0, 1, 2, \ldots, \tag{26}$$

where the orbital quantum number $l = 1$. Now, treating the mass spectral equation (20) as the unperturbed equation with the unperturbed wave functions $\phi_S(nP, \hat{q})$ for scalar mesons in Eq. (25), we now incorporate the OGE (Coulomb) term into this equation.

Then, the above mass spectral equation can be written as

$$E_S\phi_S(\hat{q}) = [-\beta_S^4\vec{\nabla}_{\hat{q}}^2 + \hat{q}^2 + V_{\text{Coul}}^S]\phi_S(\hat{q}). \tag{27}$$

Treating the Coulomb term as a perturbation to the unperturbed mass spectral equation, we can write the complete mass spectra for the ground and excited states for equal-mass heavy scalar (0^{++}) mesons using first-order perturbation theory as

$$\frac{1}{2\beta_S^2}\left\{\frac{M^2}{4} - m^2 + \frac{\beta_S^4 C_0}{\omega_0^2}\sqrt{1 + 2A_0\left(N + \frac{3}{2}\right)}\right\} + \gamma\langle V_{\text{Coul}}^S\rangle = \left(N + \frac{3}{2}\right); \quad N = 2n + l; \quad n = 0, 1, 2\ldots., \tag{28}$$

with $l = 1$, where $\langle V_{\text{Coul}}^S\rangle$ is the expectation value of V_{Coul}^S between the unperturbed states of a given quantum number n (with $l = 1$) for scalar mesons, and has been weighted by a factor of $\gamma = C_0^2\beta_S^2$ to have the Coulomb term be dimensionally consistent with the harmonic term. Its expectation values for the $1P$, $2P$, $3P$, and $4P$ states are

$$\langle 1P|V_{\text{Coul}}^S|1P\rangle = -\frac{128\pi\alpha_s}{9\beta_S^2},$$
$$\langle 2P|V_{\text{Coul}}^S|2P\rangle = -\frac{64\pi\alpha_s}{18\beta_S^2},$$
$$\langle 3P|V_{\text{Coul}}^S|3P\rangle = -\frac{3712\pi\alpha_s}{213\beta_S^2}$$
$$\langle 4P|V_{\text{Coul}}^S|4P\rangle = -\frac{1152\pi\alpha_s}{25\beta_S^2}. \tag{29}$$

We now give the mass spectrum in the BSE-CIA of the ground and excited states of χ_{c0} with quantum numbers $J^{PC} = 0^{++}$ in GeV in Tables II and III. It is seen that the set of input parameters is not unique. It is observed that the mass spectra of mesons of various J^{PC} (0^{++} in this section, and 0^{-+}, 1^{--}, 1^{++} in other sections) is somewhat insensitive to the parameter range $\omega_0 \in [0.130\text{–}0.160]$ GeV, as long as $\frac{C_0}{\omega_0^2}$ is a constant, and reasonably good fits are obtained for the parameter ratio $\frac{C_0}{\omega_0^2} = 8.8888$ GeV^{-2}, with the other parameters $\Lambda = 0.250$ GeV, $A_0 = 0.01$, and $m_c = 1.490$ GeV. Thus, for $\omega_0 = 0.130$ GeV, we have $C_0 = 0.15022$, while for $\omega_0 = 0.160$ GeV we have $C_0 = 0.227556$. (Such a relationship between two parameters that seem to be independent was also observed in Refs. [33,38]). These results for different values of ω_0 and C_0 are given in Table II. However, for comparison with experiment, we take the values $\omega_0 = 0.145$ GeV and $C_0 = 0.186889$, along with $\Lambda = 0.250$ GeV, $A_0 = 0.01$, and $m_c = 1.490$ GeV.

From the mass spectral equation, one can see that the mass spectra depend not only on the principal quantum number N, but also on the orbital quantum number l. We are now in a position to calculate the numerical values for the

TABLE III. Mass spectrum of the ground and excited states of χ_{c0} in the BSE-CIA with quantum numbers $J^{PC} = 0^{++}$ in units of GeV with the above set of parameters ($\Lambda = 0.250$ GeV, $A_0 = 0.01$, $m_c = 1.490$ GeV, $\omega_0 = 0.145$ GeV, and $C_0 = 0.186889$), along with data and the results of other models.

	BSE-CIA	Experiment [6]	Potential Models [29]	BSE [22]	RQM [30]
$M_{\chi c0}(1p_0)$	3.4474	3.4140 ± 0.0003	3.440		3.413
$M_{\chi c0}(2p_0)$	4.1552		3.9200	3.8368	3.8700
$M_{\chi c0}(3p_0)$	4.8463			4.1401	4.3010
$M_{\chi c0}(4p_0)$	5.5186				

mass spectra of heavy equal-mass scalar mesons with the input parameters of our model. The results of the mass-spectral predictions of heavy equal-mass scalar mesons for both ground and excited states with the above set of parameters is given in Table II.

We now derive the mass spectral equations with the incorporation of the OGE (Coulomb) term for pseudoscalar and vector quarkonia, and obtain their solutions in the next section (the preliminary calculations using only the confining part of the interaction were done in Ref. [48]).

IV. MASS SPECTRAL EQUATION FOR PSEUDOSCALAR (0^{-+}) AND VECTOR (1^{--}) QUARKONIA

For pseudoscalar (P), and vector (V) quarkonia, the general decomposition of the instantaneous BS wave function of dimensionality M is given in Eqs. (18) and (25), respectively, of Ref. [48]. Putting the wave function in Eq. (18) (for P-mesons) or Eq. (25) (for V-mesons) of Ref. [48] into the Salpeter equations leads to two coupled equations in the leading amplitudes (ϕ_1 and ϕ_2 for P-mesons, and χ_1 and χ_2 for V-mesons). Decoupling them in the heavy-quark limit leads Eq. (37) (for both P- and V-mesons) of Ref. [48],

$$E_{P,V}\phi_s = [-\beta_{P,V}^4\vec{\nabla}_{\hat{q}}^2 + \hat{q}^2]\phi_{P,V}(\hat{q}), \tag{30}$$

where the nonperturbative energy eigenfunctions for $l = 0(S)$ and $l = 2(D)$ states are obtained as solutions of the above spectral equation in an approximate harmonic oscillator basis for pseudoscalar quarkonia (for states $1S, \ldots, 4S$) and vector quarkonia (for states $1S, \ldots, 3D$) [as in Eq. (41) in Ref. [48]], for the perturbative calculation of the short-range one-gluon-exchange interaction shown later in this section.

The plots of unperturbed wave functions for pseudoscalar and vector quarkonia were given in Ref. [48]. The unperturbed mass spectra are expressed as (see Ref. [48])

$$\left[\frac{M^2}{4} - m^2 + \frac{\beta_{P,V}^4 C_0}{\omega_0^2}\sqrt{1 + 2A_0(N + 3/2)}\right] = 2\beta_{P,V}^2\left(N + \frac{3}{2}\right); \quad N = 2n + l; \quad n = 0, 1, 2, \ldots \tag{31}$$

The mass spectra of vector charmonium and bottomonium states using the above spectral equation was found to have degenerate S and D states [48]. However, with the incorporation of the OGE (Coulomb) term the mass spectral equation can be written as

$$E_{P,V}\phi_{P,V}(\hat{q}) = [-\beta_{P,V}^4\vec{\nabla}_{\hat{q}}^2 + \hat{q}^2 + V_{\text{Coul}}^{P,V}]\phi_{P,V}(\hat{q}). \tag{32}$$

Now, treating the Coulomb term as a perturbation to the unperturbed mass spectral equation (30), and treating the wave functions $\phi_{P,V}(\hat{q})$ in Eq. (41) of Ref. [48] as the unperturbed wave functions, we can write the complete mass spectra of ground (1S) and excited states for equal-mass heavy pseudoscalar (0^{-+}) and vector (1^{--}) mesons, respectively, using the first-order degenerate perturbation theory as

$$\frac{1}{2\beta_{P,V}^2}\left\{\frac{M^2}{4} - m^2 + \frac{\beta_{P,V}^4 C_0}{\omega_0^2}\sqrt{1 + 2A_0\left(N + \frac{3}{2}\right)}\right\} + \gamma\langle V_{\text{Coul}}^{P,V}\rangle = \left(N + \frac{3}{2}\right); \quad N = 2n + l; \quad n = 0, 1, 2\ldots, \tag{33}$$

where $\langle V_{\text{Coul}}^{P,V}\rangle$ [which again has been weighted by a factor of $\gamma_{P,V} = C_0^2\beta_{P,V}^2$, as in scalar ($0^{++}$) quarkonia in the previous section] is the matrix element of $V_{\text{Coul}}^{P,V}$ between unperturbed states in Eq. (41) of Ref. [48] for given quantum numbers n and l (with $n = 0, 1, 2, 3, \ldots$, and $l = 0$ for pseudoscalar mesons and $l = 0,\ 2$ for vector mesons). It should be noted that $V_{\text{Coul}}^{P,V}$ connects only the equal-parity states with the same quantum number n. The only nonvanishing matrix elements of the perturbation between states with the given quantum numbers n and l are listed below:

$$\langle nS|V_{\text{Coul}}^{P}|nS\rangle = \frac{\pi\alpha_s}{12}\frac{1}{\beta_P^2},$$
$$\langle nS|V_{\text{Coul}}^{V}|nS\rangle = \frac{\pi\alpha_s}{24}\frac{1}{\beta_V^2},$$
$$\langle nD|V_{\text{Coul}}^{V}|nD\rangle = \frac{\pi\alpha_s}{24}\frac{1}{5\beta_V^2}. \tag{34}$$

The nonzero values of $\langle V_{\text{Coul}}\rangle$ given above not only lead to the lifting up of the degeneracy between the S and D levels with the same principal quantum number N in vector quarkonia, but also lead to bringing the masses of different states of vector and pseudoscalar quarkonia closer to data, as can be seen from the mass spectral results for pseudoscalar (0^{-+}) and vector (1^{--}) quarkonia, which are compared with the experimental data [6] and other models for each state (where available) in Tables IV and V (for 0^{-+}) and in Tables VI and VII (for 1^{--}).

V. MASS SPECTRAL EQUATION FOR AXIAL-VECTOR 1^{++} QUARKONIA

The general form for the relativistic Salpeter wave function of the $^3P_1$ state with $J^{PC} = 1^{++}$ can be expressed as in Refs. [17,19]. Making use of the 3D reduction, and the fact that $\hat{q}.P = 0$, we can then write the general decomposition of the instantaneous BS wave function for axial-vector mesons ($J^{pc} = 1^{++}$) of dimensionality M as

TABLE IV. Masses of ground and radially excited states of η_c (in GeV) in the present calculation (BSE-CIA) along with experimental data, for a range of variations of parameter $\omega_0 \in [0.130–0.160]$ GeV for the parameter ratio $\frac{C_0}{\omega_0^2} = 8.8888$ GeV^{-2}, and the other parameters $\Lambda = 0.250$ GeV, $A_0 = 0.01$, and $m_c = 1.490$ GeV. However, for comparison with experiment, we take the value $\omega_0 = 0.145$ GeV.

	M ($\omega_0 = 0.130$)	M ($\omega_0 = 0.145$)	M ($\omega_0 = 0.160$)	Experiment [6]
$M_{\eta_c(1S)}$	3.0358	2.9759	2.9036	2.983 ± 0.0007
$M_{\eta_c(2S)}$	3.7018	3.7264	3.7484	3.639 ± 0.0013
$M_{\eta_c(3S)}$	4.4011	4.4812	4.5463	
$M_{\eta_c(4S)}$	5.0001	5.1368	5.2569	
$M_{\eta_c(5S)}$	5.570	5.7442	5.9132	

TABLE V. Masses of ground and radially excited states of η_c (in GeV) in the present calculation (BSE-CIA) along with experimental data, and their masses in other models.

	BSE-CIA	Experiment [6]	Potential Models [54]	QCD sum rule [15]	Lattice QCD [12]	[30]
$M_{\eta_c(1S)}$	2.9759	2.983 ± 0.0007	2.980	3.11 ± 0.52	3.292	2.981
$M_{\eta_c(2S)}$	3.7264	3.639 ± 0.0013	3.600		4.240	3.635
$M_{\eta_c(3S)}$	4.4812		4.060			3.989
$M_{\eta_c(4S)}$	5.1368		4.4554			4.401
$M_{\eta_c(5S)}$	5.7442					

TABLE VI. Masses of ground and radially excited states of Ψ (in GeV) in the present calculation (BSE-CIA) along with experimental data, for a a range of variations of parameter $\omega_0 \in [0.130–0.160]$ GeV for the parameter ratio $\frac{C_0}{\omega_0^2} = 8.8888$, and the other parameters $\Lambda = 0.250$ GeV, $A_0 = 0.01$, and $m_c = 1.490$ GeV. However, for comparison with experiment, we take the value $\omega_0 = 0.145$ GeV.

	M ($\omega_0 = 0.130$)	M ($\omega_0 = 0.145$)	M ($\omega_0 = 0.160$)	Experiment [6]
$M_{J/\Psi(1S)}$	3.1291	3.1017	3.0876	3.0969 ± 0.000011
$M_{\Psi(2S)}$	3.6470	3.6854	3.7163	3.6861 ± 0.00034
$M_{\Psi(1D)}$	3.6642	3.7010	3.7297	3.773 ± 0.00033
$M_{\Psi(3S)}$	4.1267	4.2135	4.2923	4.03 ± 0.001
$M_{\Psi(2D)}$	4.1643	4.2518	4.3302	4.191 ± 0.005
$M_{\Psi(4S)}$	4.5736	4.7044	4.8257	4.421 ± 0.004
$M_{\Psi(3D)}$	4.6302	4.7628	4.8854	
$M_{\Psi(5S)}$	4.9939	5.1642	5.3239	
$M_{\Psi(4D)}$	5.0673	5.2409	5.4032	

TABLE VII. Masses of ground, radially, and orbitally excited states of heavy vector quarkonium J/ψ in the BSE-CIA, along with their masses in other models and experimental data (all units are in GeV).

	BSE-CIA	Experiment [6]	Relativistic Potential Models [30]	Potential Models [54]	BSE [22]	Lattice QCD [55]
$M_{J/\psi(1S)}$	3.1017	3.0969 ± 0.000011	3.096	3.0969		3.099
$M_{\psi(2S)}$	3.6854	3.6861 ± 0.00034	3.685	3.6890	3.686	3.653
$M_{\psi(1D)}$	3.7011	3.773 ± 0.00033	3.783		3.759	
$M_{\psi(3S)}$	4.2154	4.03 ± 0.001	4.039	4.1407	4.065	4.099
$M_{\psi(2D)}$	4.2518	4.191 ± 0.005	4.150		4.108	
$M_{\psi(4S)}$	4.7044	4.421 ± 0.004	4.427	4.5320	4.344	
$M_{\psi(3D)}$	4.7628		4.507		4.371	
$M_{\psi(5S)}$	5.1642		4.837	4.8841	4.567	
$M_{\psi(4D)}$	5.2409		4.857			

$$\psi(\hat{q}) = \gamma_5\left[\gamma_\mu + \frac{P_\mu \not{P}}{M^2}\right]\left[iMg_1(\hat{q}) + \not{P} g_2(\hat{q}) - \not{\hat{q}} g_3(\hat{q}) + 2i\frac{\not{P}\not{\hat{q}}}{M} g_4(\hat{q})\right] + \gamma_5[M\hat{q}_\mu g_3(\hat{q}) + 2i\hat{q}_\mu \not{P} g_4(\hat{q})]. \tag{35}$$

With the use of our power-counting rule [25,26], it can be checked that the Dirac structures associated with the amplitudes g_1 and g_2 are $O(M^1)$ and are leading, and thus they would contribute the most to any axial-vector meson calculation. Following a similar procedure as in the case of scalar mesons, we can write the Salpeter wave function in terms of only two Dirac amplitudes: g_1 and g_2. Plugging this wave function together with the projection operators into the first two Salpeter equations in Eq. (16) of Ref. [48], and taking the trace of both sides and following the same steps as for the scalar meson case, we get the coupled integral equations in the amplitudes g_1 and g_2:

$$(M-2\omega)\left[-\frac{2mg_1}{\omega} + 2g_2\right] = \Theta_A \int \frac{d^3\hat{q}'}{(2\pi)^3} V_c(\hat{q},\hat{q}')\left[-\frac{2mg_1}{\omega} + 2g_2\right],$$
$$(M-2\omega)\left[-\frac{2mg_1}{\omega} + 2g_2\right] = -\Theta_A \int \frac{d^3\hat{q}'}{(2\pi)^3} V_c(\hat{q},\hat{q}')\left[-\frac{2mg_1}{\omega} + 2g_2\right]. \tag{36}$$

To decouple these equations, we follow a similar procedure as in the scalar meson case, and get two identical decoupled equations: one entirely in $g_1(\hat{q})$, and one entirely in $g_2(\hat{q})$. In the limit $\omega \approx m$ on the rhs, and due to the fact that for axial quarkonia again $\omega_{q\bar{q}}^4 \ll \omega_{q\bar{q}}^2$, these equations can be expressed as

$$\left[\frac{M^2}{4} - m^2 - \hat{q}^2\right] g_1(\hat{q}) = -m\Theta_A\omega_{q\bar{q}}^2\left[\vec{\nabla}_{\hat{q}}^2 + \frac{C_0}{\omega_0^2}\right] g_1(\hat{q}),$$
$$\left[\frac{M^2}{4} - m^2 - \hat{q}^2\right] g_2(\hat{q}) = -m\Theta_A\omega_{q\bar{q}}^2\left[\vec{\nabla}_{\hat{q}}^2 + \frac{C_0}{\omega_0^2}\right] g_2(\hat{q}), \tag{37}$$

where it can be checked that both g_1 and g_2 satisfy the same equation, and hence we can approximately write $g_1 \sim g_2 \sim \phi_A$. Thus,

$$\left[\frac{M^2}{4} - m^2 - \hat{q}^2\right]\phi_A(\hat{q}) = -\Theta_A m\omega_{q\bar{q}}^2\left[\vec{\nabla}_{\hat{q}}^2 + \frac{C_0}{\omega_0^2}\right]\phi_A(\hat{q}), \tag{38}$$

where $\Theta_A = \gamma_\mu\Psi(\hat{q})\gamma_\mu$. Now, with the use of leading Dirac structures, we can again to a good approximation express $\Theta_A = 2$. This is due to the fact that $\gamma_\mu\psi(\hat{q})\gamma_\mu \approx \gamma_\mu\gamma_5\gamma_\nu(iMg_1)\gamma_\mu = 2\gamma_5\gamma_\nu(iMg_1) \approx 2\psi(\hat{q})$. This mass spectral equation has the same form as the mass spectral equation for scalar quarkonia [Eq. (18)], except for the value of Θ_A, which is different from Θ_S. Thus, the above equation can be put in a similar form as Eq. (20) (for the scalar case), except that the inverse range parameter $\beta_s \to \beta_A$, where $\beta_A = (\frac{2m\omega_{q\bar{q}}^2}{\sqrt{1+2A_0(N+3/2)}})^{1/4}$, and the $3D$ wave function $\phi_s \to \phi_A$. The mass spectral equation for 1^{++} would then exactly resemble Eq. (20) for the 0^{++} case, and thus the unperturbed wave functions $\phi_A(\hat{q})$ for 1^{++} would then have the same algebraic form as $\phi_s(\hat{q})$ in Eq. (25), but with $\beta_s \to \beta_A$:

$$\phi_A(1p,\hat{q}) = \left(\frac{2}{3}\right)^{1/2}\frac{1}{\pi^{3/4}\beta_A^{5/2}}\hat{q}e^{-\frac{\hat{q}^2}{2\beta_A^2}},$$
$$\phi_A(2p,\hat{q}) = \left(\frac{5}{3}\right)^{1/2}\frac{1}{\pi^{3/4}\beta_A^{5/2}}\hat{q}\left[1 - \frac{2}{5}\frac{\hat{q}^2}{\beta_A^2}\right]e^{-\frac{\hat{q}^2}{2\beta_A^2}},$$
$$\phi_A(3p,\hat{q}) = \left(\frac{70}{171}\right)^{1/2}\frac{1}{\pi^{3/4}\beta_A^{5/2}}\hat{q}\left[1 - \frac{2\hat{q}^2}{5\beta_A^4} + \frac{4\hat{q}^4}{35\beta_A^4}\right]e^{-\frac{\hat{q}^2}{2\beta_A^2}},$$
$$\phi_A(4p,\hat{q}) = \left(\frac{1890}{46359}\right)^{1/2}\frac{1}{\pi^{3/4}\beta_A^{5/2}}\hat{q}\left[1 - \frac{6\hat{q}^2}{5\beta_A^2} + \frac{12\hat{q}^4}{35\beta_A^4} - \frac{24\hat{q}^6}{945\beta_A^6}\right]e^{-\frac{\hat{q}^2}{2\beta_A^2}}. \tag{39}$$

The plots of the wave functions for axial-vector quarkonia are given in Fig. 2.

Now, the perturbative inclusion of the Coulomb term will reduce mass spectrum for axial-vector meson in the same form as Eqs. (27)–(29) for the scalar case, except that the inverse range parameter β_s must be replaced by β_A. The complete mass spectral equation for ground and excited states of 1^{++} is

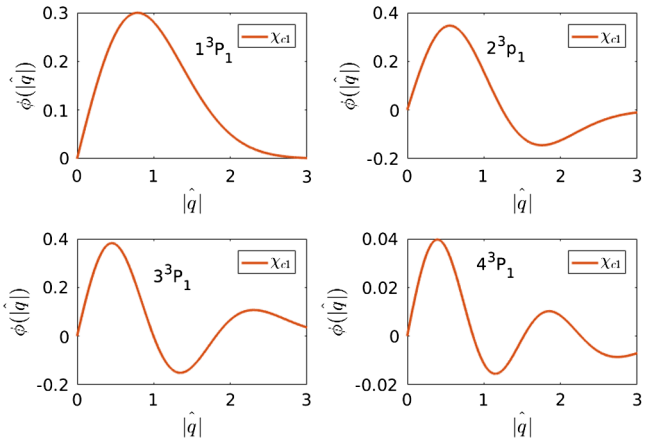

FIG. 2. Plots of wave functions for axial-vector (1^{++}) quarkonia χ_{c1} Vs $\hat{q}$ (in GeV) for the states $1P$, $2P$, and $3P$.

$$E_A\phi_A(\hat{q}) = [-\beta_A^4\vec{\nabla}_{\hat{q}}^2 + \hat{q}^2 + V_{\rm Coul}^A]\phi_A(\hat{q}). \quad (40)$$

The solutions of the above spectral equation are

$$\frac{1}{2\beta_A^2}\left\{\frac{M^2}{4} - m^2 + \frac{\beta_A^4 C_0}{\omega_0^2}\sqrt{1 + 2A_0\left(N + \frac{3}{2}\right)}\right\} + \gamma_A\langle V_{\rm Coul}^A\rangle = \left(N + \frac{3}{2}\right); \quad N = 2n + l; \quad n = 0, 1, 2\ldots, \quad (41)$$

with $l = 1$, where $\langle V_{\rm Coul}^A\rangle$ is the expectation value of $V_{\rm Coul}^A$ between the unperturbed states of a given quantum number n (with $l = 1$) for axial-vector mesons, which has been weighted by a factor of $\gamma_A = C_0^2\beta_A^2$ to make the Coulomb term dimensionally consistent with the harmonic term. Its expectation values for the $1P$, $2P$, and $3P$ states are

$$\langle 1P|V_{\rm Coul}^A|1P\rangle = -\frac{64\pi\alpha_s}{9\beta_A^2},$$
$$\langle 2P|V_{\rm Coul}^A|2P\rangle = -\frac{32\pi\alpha_s}{18\beta_A^2},$$
$$\langle 3P|V_{\rm Coul}^A|3P\rangle = -\frac{1856\pi\alpha_s}{213\beta_A^2},$$
$$\langle 4P|V_{\rm Coul}^A|4P\rangle = -\frac{576\pi\alpha_s}{25\beta_A^2}. \quad (42)$$

From the mass spectral equation one can see that the mass spectra again depend on both the principal quantum number N and the orbital quantum number l. We are now in a position to calculate the numerical values for the mass spectra of heavy scalar quarkonia with the input parameters of our model. The results of the mass spectral predictions of heavy equal-mass scalar mesons for both ground and excited states with the above set of parameters are given in Table II. The results for the masses of ground ($1P$) and excited ($2P$ and $3P$) states of quarkonia χ_{c1} are given in Table VIII and IX.

VI. TWO-PHOTON DECAYS OF SCALAR QUARKONIUM

We now study the two-photon decay width of scalar quarkonium (0^{++}), which proceeds through the quark-triangle diagrams shown in Fig. 3.

Let P be the total momentum of the scalar quarkonia, and $k_{1,2}$ be the momenta of the two emitted photons with polarizations $\varepsilon_{1,2}$, respectively. Then we can write $P = k_1 + k_2$, and let $2Q = k_1 - k_2$. The invariant amplitude for this process can be written as

TABLE VIII. Mass spectrum in the BSE-CIA of ground and excited states of χ_{c1} with quantum numbers $J^{PC} = 1^{++}$ in units of GeV with a range of variations of parameter $\omega_0 \in [0.130 - 0.160]$ GeV for the parameter ratio $\frac{C_0}{\omega_0^2} = 8.8888$ GeV^{-2}, and the other parameters $\Lambda = 0.250$ GeV, $A_0 = 0.01$, and $m_c = 1.490$ GeV. However, for comparison with experiment, we take the value $\omega = 0.145$ GeV.

	M ($\omega_0 = 0.130$)	M ($\omega_0 = 0.145$)	M ($\omega_0 = 0.160$)	Experiment [6]
$M_{\chi c1}(1p_1)$	3.4370	3.4782	3.5279	3.510 ± 0.0007
$M_{\chi c1}(2p_1)$	3.9279	3.9560	4.0333	$3.871.69 \pm 0.0017$
$M_{\chi c1}(3p_1)$	4.3858	4.4650	4.6636	
$M_{\chi c1}(4p_1)$	4.8155	4.9593	5.3151	

TABLE IX. Mass spectrum of ground and excited states of χ_{c1} with quantum numbers $J^{PC} = 1^{++}$ in units of GeV with the set of parameters $\omega_0 = 0.145$ GeV, $C_0 = 0.186889$, $A_0 = 0.01$, and $m_c = 1.490$ GeV.

	BSE-CIA	Experiment [6]	Potential Models [29]	BSE [22]	RQM [30]
$M_{\chi c1}(1p_1)$	3.4783	3.510 ± 0.0007	3.440		3.413
$M_{\chi c1}(2p_1)$	3.9560	$3.871.69 \pm 0.0017$	3.920	3.928	3.870
$M_{\chi c1}(3p_1)$	4.4650			4.228	4.301
$M_{\chi c1}(4p_1)$	4.9593				

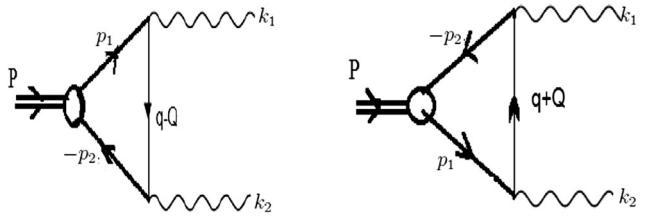

FIG. 3. Diagrams contributing to the two-photon decays of scalar (0^{++}) quarkonia.

$$M_{fi}(S\to\gamma\gamma)=\frac{i\sqrt{3}(ie_Q)^2}{m^2+\frac{M^2}{4}}\int\frac{d^3\hat{q}}{(2\pi)^3}\mathrm{Tr}[\Psi^s(\hat{q}) \times[\not\epsilon 1(m+i\not{Q})\not\epsilon 2+\not\epsilon 2(m+i\not{Q})\not\epsilon 1]], \quad (43)$$

where $e_Q=+\frac{2}{3}e$ for $c\bar{c}$. The 3D structure of the Dirac wave function $\Psi^s(\hat{q})$ is given in Eqs. (9) and (17). The propagators for the third quark in the two diagrams is expressed as $S_F(q\mp Q)=\frac{-i(\not{q}\mp\not{Q})+m}{(q\mp Q)^2+m^2}$. Now, for heavy hadrons—where the system can be regarded as nonrelativistic—it is a good approximation to take the internal momentum $q\ll M$, and, hence, $q^2\ll Q^2$, where it can be seen that $Q^2=\frac{M^2}{4}$. Using the propagator expressions given above, and evaluating the trace over the gamma matrices, we can write the invariant amplitude given above as

$$M_{fi}(S\to\gamma\gamma)=(\epsilon_1.\epsilon_2)F_S,$$
$$F_S=\left(\frac{16\alpha_{em}}{3\sqrt{3}\pi^2}\right)\frac{mM}{m^2+\frac{M^2}{4}}\int d^3\hat{q}\phi_s(\hat{q}), \quad (44)$$

where F_S is the decay constant for scalar quarkonium χ_{c0}. The decay width for the process can then be expressed as

$$\Gamma(S\to\gamma\gamma)=\frac{1}{32\pi M}|F_S|^2. \quad (45)$$

For the lowest 0^{++} states, we obtain $\Gamma_{\chi_{c0}(1p_1)\to\gamma\gamma}=2567.06$ eV (Expt $=2341.50$ eV [6]), and $\Gamma_{\chi_{c0}(2p_1)\to\gamma\gamma}=1376.20$ eV (for which data is not yet available). However there are very large variations in results of two-photon decay widths in various models (see Ref. [29,56,57].

VII. DISCUSSIONS

We have employed a 3D reduction of the BSE [with a 4×4 representation for the two-body ($q\bar{q}$) BS amplitude] under the CIA to derive the algebraic forms of the mass spectral equations for scalar, pseudoscalar, vector, and axial-vector quarkonia using the full BS kernel comprised of the one-gluon-exchange and the confining part in an approximate harmonic oscillator basis, which led to analytic solutions (both eigenfunctions and eigenvalues). We thus obtained the mass spectra of $c\bar{c}$ quarkonia for the ground and excited states of 0^{++}, 0^{-+}, 1^{--}, and 1^{++} states. The mass spectral results for all of these states—which were compared with the experimental data [6] and other models for each state (where available)—are given in Tables II–IX respectively. The masses and the algebraic forms of the eigenfunctions for each quarkonium state so obtained will be used to calculate their various transitions.

As mentioned in Sec. II, in this work the partitioning of relativistic internal momentum q comes from the Wightman-Garding definitions $\hat{m}_{1,2}$ of the masses of individual quarks (explained in detail in Sec. II). Hence, for equal-mass quarkonia (such as $c\bar{c}$ studied in this work) we get $p_{1,2}=\frac{1}{2}P\pm q$ (as in Refs. [37,38]), and the momentum is shared equally between the two quarks, which is a logical choice. However, for unequal-mass mesons (where $m_1\neq m_2$) the $\hat{m}_{1,2}$ allocate most of the momentum to the heavy quark, while a smaller part of the momentum is allocated to the lighter quark (such that the relation $\hat{m}_1+\hat{m}_2=1$ is always satisfied), which is a reasonable choice in a heavy-light meson. But this choice is not needed in a Poincaré-covariant formulation of the amplitudes [39,40], where one could use, in general, $p_1=q+\alpha P$ and $p_2=-q+(1-\alpha)P$, where the momentum partitioning parameter $\alpha\in[0,1]$ and is arbitrary, and the numerical results for the amplitudes and masses are independent of α. Its arbitrariness is equivalent to a freedom in the definition of the quark-antiquark relative momentum, since in a Poincaré-covariant formulation no physical observable should depend on the choice of momentum partitioning. Hence, even though the 3D reduction through the CIA employed by us makes our formulation relativistically covariant, it may not be Poincaré covariant since our results depend on the choice of internal momentum. To have both Lorentz and Poincaré covariance, the full 4D structure of the BS amplitudes has to be used. With the omission of the full structure of amplitudes comes the complication that the results can be sensitive to the definition of the relativistic internal momentum (see Ref. [42]). This may also be due to the numerical approximations used.

We wish to mention that, in principle, in $Q\bar{Q}$ quarkonia the constituents are close enough to each other to warrant a more accurate treatment of the Coulomb term. Though for $b\bar{b}$ systems the Coulomb term will be extremely dominant in comparison to the confining term, it may not be so unreasonable to treat the Coulomb term perturbatively for $c\bar{c}$ systems. Here we wish to point out that if we get reasonable results for orbital $c\bar{c}$ excitations, it is mainly due to centrifugal effects [43] which ensure that the $c-\bar{c}$ separation is large enough to feel the effect of the confining term more strongly than the Coulomb term. Further, the present approach is in line with some earlier works [43–45] where the OGE (Coulomb) term was treated perturbatively for charmed mesons and baryons. Similarly, in a recent work [46] the 3D harmonic oscillator wave functions were used as trial wave functions for obtaining the $c\bar{c}$ spectrum and their decays, where these trial wave functions did not take into account the importance of the Coulomb potential for heavy quarkonium systems. A similar treatment was followed earlier in Ref. [47].

Also, in a recent work [48] in which one of us was involved, we did not take into account the Coulomb interactions between $c\bar{c}$ and $b\bar{b}$ states, and used only the confining interaction to study their spectra and decays, in line with other works [49–51].

However, in the present approach (using only the confining interactions) we first analytically derived the algebraic forms of the wave functions for various $c\bar{c}$ states, which are in the form of harmonic oscillators. Though we then introduced the Coulomb term perturbatively for $c\bar{c}$ (and not for $b\bar{b}$), this present calculation is a substantial improvement over our previous work in Ref. [48] (where we did not treat the Coulomb interaction at all). However, for $b\bar{b}$ states, a more exact nonperturbative treatment of the Coulomb interaction would be needed.

Further, our results for the $c\bar{c}$ mass spectra suggest that the perturbative incorporation of OGE with the use of analytically derived harmonic oscillator wave functions is closer to reality than some of the previous approaches [46,47], where they used harmonic oscillator wave functions only as trial wave functions, which did not take into account the importance of the Coulomb potential for heavy quarkonium systems.

All numerical calculations have been done using MATHEMATICA. We selected the best set of five input parameters [given after Eq. (16)] that gave reasonable matching with data for the masses of the ground and excited states of $c\bar{c}$ quarkonia for 0^{++}, 0^{-+}, 1^{--}, and 1^{++} states. It was seen that this set of input parameters is not unique. It was observed that the mass spectra of mesons of various J^{PC} is somewhat insensitive (as can be seen from Tables II–VIII) to a range of variations of parameter $\omega_0 \in [0.130\text{–}0.160]$ GeV as long as $\frac{C_0}{\omega_0^2}$ is a constant, and reasonably good fits are obtained for the parameter ratio $\frac{C_0}{\omega_0^2} = 8.8888\ \text{GeV}^{-2}$, with the other parameters $\Lambda = 0.250$ GeV, $A_0 = 0.01$, and $m_c = 1.490$ GeV. Thus, for $\omega_0 = 0.130$ GeV we have $C_0 = 0.15022$, while for $\omega_0 = 0.160$ GeV we have $C_0 = 0.227556$. (Such a relationship between two parameters that seem to be independent was also observed in Refs. [33,38].) However, for comparison with experiment, we took the values $\omega = 0.145$ GeV, and $C_0 = .186889$, along with $\Lambda = 0.250$ GeV, $A_0 = 0.01$, and $m_c = 1.490$ GeV. It was seen that only the lowest states (ground and one or two excited states) have reasonable fits. However, the disagreement with experiment increases as one goes to higher excited states. The analytic forms of the wave functions derived for 0^{++} states of $c\bar{c}$ were employed to calculate their two-photon decays.

We wish to also point out that the present calculation with perturbative incorporation of the one-gluon-exchange interaction lifts up the degeneracy between the S and D states of vector quarkonia, and also gives a better agreement with the data for these states. The results obtained for the ground $(1P)$ state of χ_{c0}, as well as the ground and first excited states of χ_{c1}, are in reasonable agreement with data. However, there are open questions about the quantum number assignments of the state $X(3915)$, which are available in Particle Data Group tables. Some authors [7,8] have argued that it is difficult to assign $X(3915)$ to $\chi_{c0}(2P)$, and that it could be $\chi_{c2}(2P)$. The possible mass of $\chi_{c0}(2P)$ was recently predicted in Ref. [7] as 3.837 ± 0.0115 MeV. We then worked out the decay widths of χ_{c0} for the ground $(1P)$ and excited $(2P)$ states, and compared our results with data and other models in Table VI. Though our results are smaller than data [6], they compare roughly other models [56,57]. Further, a large variation in the decay widths can be seen in other models.

However, as mentioned earlier, our main emphasis in this paper was to show that this problem of the 4×4 BSE under the heavy-quark approximation can indeed be handled analytically for both the masses and wave functions of radially and orbitally excited states. In this framework, from the beginning, we employed a 4×4 representation for the two-body $(q\bar{q})$ BS amplitude to calculate both the mass spectra and the transition amplitudes. However, the price we had to pay was to solve a coupled set of equations for scalar, pseudoscalar, vector, and axial-vector quarkonia, which we have explicitly shown get decoupled in the heavy-quark approximation $(\omega \approx m)$, leading to a mass spectral equation with analytical solutions for both masses—as well as eigenfunctions for all of the above states—in an approximate harmonic oscillator basis. The analytical forms of the eigenfunctions for ground and excited states so obtained can be used to calculate various transitions of these quarkonia.

The heavy-quark approximation for quarkonia is valid because not only is the relative momentum between heavy quarks in the bound states considered small, but also these quarks are treated as almost on mass shell [53], which is justified for the calculation of low-energy properties like the mass spectrum and the decays of quarkonia ($c\bar{c}$ systems). This approximation, is well under control, in the context of heavy quark systems.

We further wish to point out that this analytic approach (giving an explicit dependence of the spectra on the principal quantum number N) under the heavy-quark approximation gives much deeper insight into the spectral problem than the purely numerical approaches prevalent in the literature. The plots of the analytical forms of wave functions for various J^{PC} states (obtained as solutions of their mass spectral equations) are also given in Figs. 1 and 2 for scalar and axial-vector quarkonia. The correctness of our approach can be gauged by the fact that these plots are very similar to the corresponding plots of amplitudes for these quarkonia in Ref. [22] obtained by purely numerical methods. The analytical forms of the eigenfunctions for ground and excited states so obtained can be used to evaluate the various other processes involving

scalar and axial-vector quarkonia, which we intend to do next.

ACKNOWLEDGMENTS

This work was carried out at Addis Ababa University, Ethiopia, and at Chandigarh University, India. The authors wish to thank both institutions for the facilities provided during the course of this work. One of us (L. A.) wishes to thank Samara University, Ethiopia for support for his doctoral program. He also wishes to thank Chandigarh University for the hospitality during his visit during August–October 2017.

[1] N. Brambilla, A. Pineda, J. Soto, and A. Vairo, Rev. Mod. Phys. **77**, 1423 (2005).
[2] K. M. Ecklund *et al.* (CLEO Collaboration), Phys. Rev. D **78**, 091501 (2008).
[3] B. Auger *et al.* (*BABAR* Collaboration), Phys. Rev. Lett. **103**, 161801 (2009).
[4] K. F. Chen *et al.* (Belle Collaboration), Phys. Rev. D **82**, 091106(R) (2010).
[5] K. W. Edwards *et al.* (CLEO Collaboration), Phys. Rev. Lett. **86**, 30 (2001).
[6] K. A. Olive *et al.* (Particle Data Group), Chin. Phys. C **38**, 090001 (2014).
[7] F. K. Guo and U.-G. Meisner, Phys. Rev. D **86**, 091501 (2012).
[8] S. L. Olsen, Phys. Rev. D **91**, 057501 (2015).
[9] N. Brambilla *et al.*, Eur. Phys. J. C **71**, 1534 (2011).
[10] C. McNielle, C. T. H. Davies, E. Follana, K. Hornbostel, and G. P. Lepage (HPQCD Collaboration), Phys. Rev. D **86**, 074503 (2012).
[11] G. S. Bali, K. Schiling, and A. Wachter, Phys. Rev. D **56**, 2566 (1997).
[12] T. Burch, C. DeTar, M. Di Pierro, A. X. El-Khadra, E. D. Freeland, S. Gottlieb, A. S. Kronfeld, L. Levkova, P. B. Mackenzie, and J. N. Simone (Fermilab and MILC Collaboration), Phys. Rev. D **81**, 034508 (2010).
[13] J. Gasser and H. Leutwyler, Ann. Phys. (N.Y.) **158**, 142 (1984).
[14] M. A. Shifman, A. I. Vainshtein, and V. I. Zakharov, Nucl. Phys. **B147**, 385, 448 (1979).
[15] E. Veli Veliev, K. Azizi, H. Sundu, and N. Aksit, J. Phys. G **39**, 015002 (2012).
[16] G. T. Bodwin, E. Braaten, and G. P. Lepage, Phys. Rev. D **51**, 1125 (1995).
[17] C. H. L. Smith, Ann. Phys. (N.Y.) **53**, 521 (1969).
[18] A. N. Mitra and B. M. Sodermark, Nucl. Phys. **A695**, 328 (2001).
[19] R. Alkofer and L. W. Smekel, Phys. Rep. **353**, 281 (2001).
[20] H. J. Munczek and P. Jain, Phys. Rev. D **46**, 438 (1992).
[21] C. S. Kim and G. L. Wang, Phys. Lett. B **584**, 285 (2004).
[22] C.-H. Chang and G. L. Wang, Sci. China G **53**, 2005 (2010).
[23] A. N. Mitra and S. Bhatnagar, Int. J. Mod. Phys. A **07**, 121 (1992).
[24] S. Bhatnagar, D. S. Kulshreshtha, and A. N. Mitra, Phys. Lett. B **263**, 485 (1991).
[25] S. Bhatnagar and S.-Y. Li, J. Phys. G **32**, 949 (2006).
[26] S. Bhatnagar, S-Y. Li, and J. Mahecha, Int. J. Mod. Phys. E **20**, 1437 (2011).
[27] S. Bhatnagar, J. Mahecha, and Y. Mengesha, Phys. Rev. D **90**, 014034 (2014).
[28] H. Negash and S. Bhatnagar, Adv. High Energy Phys. **2017**, 7306825 (2017).
[29] S. Godfrey and N. Isgur, Phys. Rev. D **32**, 189 (1985).
[30] D. Ebert, R. N. Faustov, and V. O. Galkin, Phys. At. Nucl. **76**, 1554 (2013); Eur. Phys. J. C **71**, 1825 (2011).
[31] S. Patel, P. C. Vinodkumar, and S. Bhatnagar, Chin. Phys. C **40**, 053102 (2016).
[32] E. Rojas, B. El-Bennich, and J. P. B. C. de Melo, Phys. Rev. D **90**, 074025 (2014).
[33] F. F. Mojica, C. E. Vera, E. Rojas, and B. El-Bennich, Phys. Rev. D **96**, 014012 (2017).
[34] M. Blank and A. Krassnigg, Phys. Rev. D **84**, 096014 (2011).
[35] C. S. Fischer, S. Kubrak, and R. Williams, Eur. Phys. J. A **51**, 10 (2015).
[36] M. Ding, F. Gao, L. Chang, Y. X. Liu, and C. D. Roberts, Phys. Lett. B **753**, 330 (2016).
[37] T. Hilger, C. Popovici, M. Gmez-Rocha, and A. Krassnigg, Phys. Rev. D **91**, 034013 (2015).
[38] T. Hilger, M. Gmez-Rocha, and A. Krassnigg, Phys. Rev. D **91**, 114004 (2015).
[39] M. A. Bedolla, J. J. Cobos-Martnez, and A. Bashir, Phys. Rev. D **92**, 054031 (2015).
[40] M. A. Bedolla, K. Raya, J. J. Cobos-Martnez, and A. Bashir, Phys. Rev. D **93**, 094025 (2016).
[41] F. E. Serna, B. El-Bennich, and G. Krein, Phys. Rev. D **96**, 014013 (2017).
[42] B. E. Bennich, M. A. Paracha, C. D. Roberts, and E. Rojas, Phys. Rev. D **95**, 034037 (2017).
[43] A. N. Mitra and I. Santhanam, Z. Phys. C **8**, 33 (1981).
[44] A. Majethiya, B. Patel, A. K. Rai, and P. C. Vinodkumar, arXiv:0809.4910.
[45] F. Arleo, J. Cugnon, and Y. Kalinovsky, Phys. Lett. B **614**, 44 (2005).
[46] Bhaghyesh and K. B. Vijayakumar, Chin. Phys. C **37**, 023103 (2013).
[47] S. Capstick and S. Godfrey, Phys. Rev. D **41**, 2856 (1990).
[48] H. Negash and S. Bhatnagar, Int. J. Mod. Phys. E **25**, 1650059 (2016).
[49] R. Ricken, M. Koll, D. Merten, B. Metsch, and H. Petry, Eur. Phys. J. A **9**, 221 (2000).
[50] T. Babutsidze, T. Kopaleishvili, and A. Rusetsky, Phys. Rev. C **59**, 976 (1999).
[51] M. G. Olsson, A. D. Martin, and A. W. Peacock, Phys. Rev. D **31**, 81 (1985).

[52] C. B. Yang and X. Cai, Phys. Rev. D **51**, 6332 (1995).
[53] S. Bhatnagar, M. Li, and S.-Y. Li, J. Mod. Phys. **05**, 1027 (2014).
[54] Bhagyesh, K. B. V. Kumar, and A. P. Monterio, J. Phys. G **38**, 085001 (2011).
[55] T. Kawanai and S. Sasaki, AIP Conf. Proc. **1701**, 050022 (2016).
[56] C. R. Munz, Nucl. Phys. **A609**, 364 (1996).
[57] D. Ebert, R. N. Faustov, and V. O. Galkin, Mod. Phys. Lett. A **18**, 601 (2003).